

The hydrodynamic modelling of torque converters

by P. J. Strachan,* F. P. Reynaud,** and T. W. von Backström,***

(Received in final form November 1991)

List of Symbols

B	factor used in calculation of Y_k
c	blade chord length (m)
C_w	tangential component of absolute fluid velocity corresponding to β (m/s)
d	minimum opening between blades (m)
D	NACA diffusion factor
D_h	hydraulic diameter (m)
H	blade height (m)
i	incidence angle ($^\circ$)
i_s	stall incidence angle ($^\circ$)
k	casing friction loss coefficient, or V_1/V_2
k_e	tip clearance (m)
k_s	height of surface roughness asperities (m)
\dot{m}	mass flow rate (kg/s)
r	blade radius (m)
p_s	static pressure (Pa)
p_t	total pressure (Pa)
Re	Reynold's number
Re_c	casing Reynold's number
s	blade inlet pitch (m)
t	blade thickness (m)
U	blade tip speed (m/s)
V	relative fluid velocity (m/s)
V_w	tangential component of relative fluid velocity (m/s)
Y_k	tip clearance loss coefficient
Y_p	primary or profile loss coefficient
Y_s	secondary loss coefficient
Z_l	blade loading
Z_n	number of blades
α	absolute inlet flow angle ($^\circ$)
α_d	blade inlet angle ($^\circ$)
α_m	mean flow angle ($^\circ$)
β	absolute outlet flow angle ($^\circ$)
β_d	blade outlet angle ($^\circ$)
δ	shock loss coefficient
ΔC_w	$C_{w2} - C_{w1}$ (m/s)
ΔV_w	difference between actual and design V_w (m/s)
ϵ	half blade width, see fig. 9, (m)
ϵ_{Lim}	limiting radius ratio
ρ	fluid density (kg/m ³)
σ	slip factor
Λ	impeller friction factor

Subscript Notation

1	inlet
2	outlet

* Senior Lecturer,
 ** M.Eng. Student,
 *** Professor, Member
 Department of Mechanical Engineering,
 University of Stellenbosch

Summary

One method of predicting the performance characteristics of torque converters is by means of a hydrodynamic model in which the geometry of the torque converter and the properties of the fluid are given, and the angular momentum flux over the members is calculated at specific operating points. A number of such models has been developed in the literature, all of which rely on empirical input data for determination of the losses and slip factor. This paper describes a hydrodynamic model in which the empiricism has been removed from the input data and built into the program in the form of empirical equations and loss models. The program can be applied to torque converters having profile and thin blades, and in addition a new shock (incidence) loss model is introduced which is employed in the hydrodynamic model to calculate the shock losses of the different members of a torque converter. Prediction of torque converter performance by means of this model agreed well with published experimental data for a wide range of torque converter geometries.

Introduction

Torque converters are widely used in automotive applications, from passenger cars to heavy commercial and military vehicles. The primary function of the torque converter is to provide torque multiplication. This is a maximum at stall and decreases without step to a value of

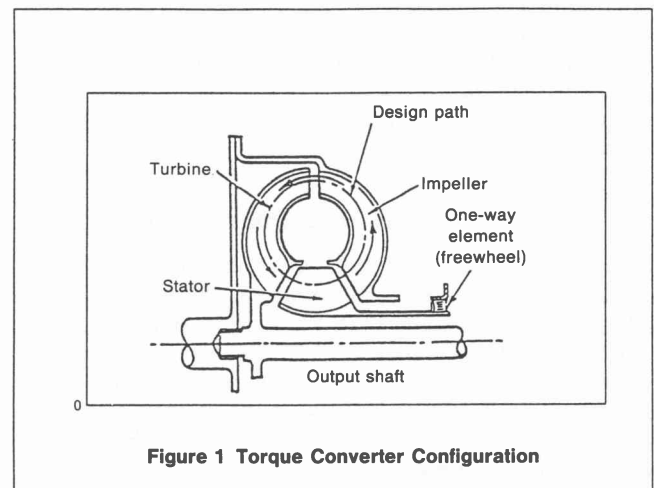


Figure 1 Torque Converter Configuration

unity at the coupling point. The configuration of a typical torque converter is shown in fig. 1 [1]. The torque converter is similar to a fluid coupling, but with the addition of a stator or reactor. In a fluid coupling, power is transmitted from the pump or impeller to the turbine without change in torque, but with the insertion of the stator in the circuit, the angular momentum of the fluid is changed between the turbine exit and impeller entrance, resulting in torque multiplication between impeller and turbine. As

its name implies, the stator is normally stationary but in most modern torque converters it is usually fitted with a one-way clutch.

The characteristic performance curves of torque converters and fluid couplings are shown in fig. 2. The abscissa is speed ratio, the ratio of output (or turbine) speed to input (or impeller) speed. The ordinates are torque ratio i.e. output torque to input torque on the one side and efficiency on the other.

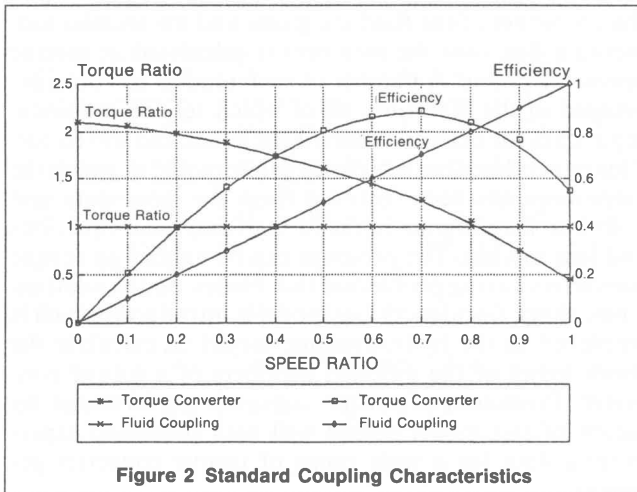


Figure 2 Standard Coupling Characteristics

Between speed ratios of 0.8 and 0.9, the converter torque curve crosses that of the coupling, indicating that the turbine (or output) torque is less than the impeller (or input torque). Simultaneously the converter efficiency drops below that of the coupling. As this is not desirable, it is overcome either by the fitting of a one way clutch, or by the use of a mechanical lock-up device that automatically connects the impeller and turbine above the speed ratio that corresponds to a torque ratio of unity.

This paper describes a comprehensive one dimensional model to simulate accurately the flow processes in a torque converter and predict the performance characteristics.

Torque Converter Hydrodynamic Models

In the torque converter and fluid coupling field one dimensional models are fairly common. Lucas and Rayner [2], Qualman and Egbert [3], Walker [4], Whitfield, Wallace and Patel [5], Wallace, Whitfield and Sivalingam [6], Lamprecht [7] and Adrian [8], have all produced one dimensional models which show more or less agreement with measured results, but all of these require the external specification of total pressure loss coefficients for the members (pump impeller, turbines and stators) and of blade incidence loss coefficients. Lamprecht [7] did however derive equations for the calculation of certain of the loss coefficients, but they were not implemented in the computer program listing of his thesis [7].

With the local availability of the Lamprecht [7] model, it was decided to utilise it as the basis for further development. The Lamprecht [7] model was obtained and completely re-written in the BASIC language to run on a standard IBM compatible personal computer. In the analysis,

the input speed, the speed ratio and the geometry of the torque converter are given parameters. There are three main members, the impeller, the stator and the turbine, although each can have more than one stage. The stator in turn can have two phases of operation, namely fixed or freewheel. Further assumptions are;

- steady state conditions throughout
- incompressible fluid
- work done by the fluid is positive and work received by the fluid is negative
- conservation of mass flow, momentum and energy
- the torque applied to the shell is not considered

The process estimates a mass flow inside the torus and this is used to determine firstly, the torque and power transmitted (input power) and absorbed (output power) by the members and, secondly, the power losses due to friction, diffusion, shock and slip.

For conservation of energy, the sum of the input power, output power and power losses, bearing in mind the sign convention, must equate to zero, and the mass flow is then iteratively adjusted until this condition, or close to it, is achieved. The value of mass flow thus derived is then used to determine the input and output torques, torque ratio, and efficiency for different values of speed ratio. In calculating the power losses, values of the stagnation pressure loss coefficients for the impeller, stator and turbine, the shock (or incidence) loss factors and the impeller slip factor are required. At this stage values based on information in the literature were assumed, typically 0,35 for the loss coefficients, and 1,0 for the shock loss and slip factors. Wall friction losses were ignored.

Evaluation of the Initial Model with Externally Specified Loss Coefficients

An extensive series of computer tests was run on the standard Jandasek [9] torque converter geometry. Fig. 3 shows good agreement between calculated and measured torque ratio and efficiency using the loss coefficients and factors above, with maximum differences, as can be seen from Table 1, of about 3%. However, from fig. 4 it can be seen that only qualitative agreement was obtained be-

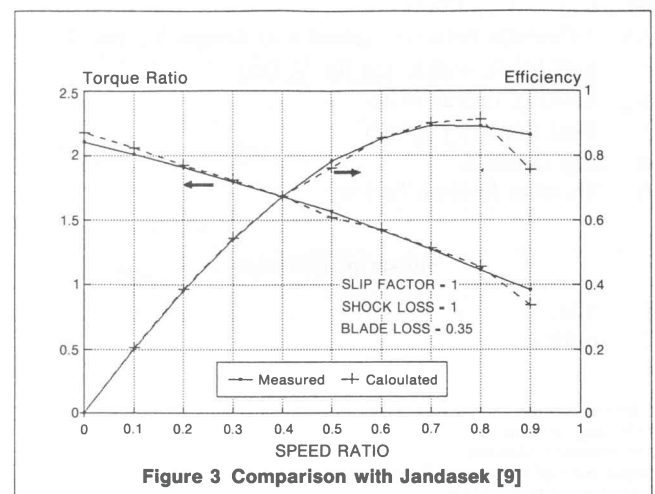


Figure 3 Comparison with Jandasek [9]

(a) Figs. 3 and 4

Torque Ratio			Input Torque ft lbs			Output Torque ft lbs		
Meas	Calc	Diff %	Meas	Calc	Diff %	Meas	Calc	Diff %
2,11	2,18	3,4	348	415	19,3	733	905	23,4
2,01	2,06	2,5	346	406	17,4	696	838	20,3
1,91	1,93	1,0	336	397	17,9	643	766	19,1
1,80	1,81	0,7	325	383	17,9	585	694	18,7
1,68	1,68	0,0	309	367	18,8	520	617	18,7
1,56	1,55	0,7	288	348	21,0	450	541	20,1
1,42	1,42	0,2	264	322	21,9	376	459	22,2
1,27	1,29	1,1	237	290	22,5	302	374	23,8
1,11	1,14	2,4	204	248	21,6	227	283	24,5
0,96	0,99	3,0	167	186	11,1	160	183	14,5
Ave. diff %		1,5	Ave. diff %		19,0	Ave. diff %		20,5
Std. dev.		1,1	Std. dev.		3,1	Std. dev.		2,9

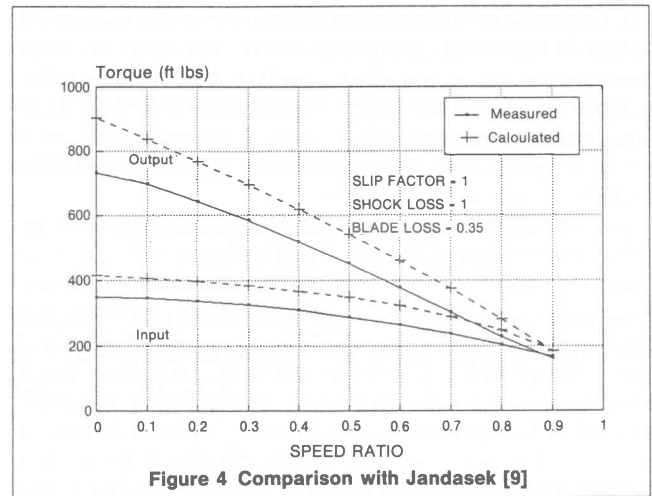
(b) Figs. 10 and 11

Torque Ratio			Input Torque ft lbs			Output Torque ft lbs		
Meas	Calc	Diff %	Meas	Calc	Diff %	Meas	Calc	Diff %
2,11	2,20	4,6	348	341	2,0	733	752	2,5
2,01	2,07	2,8	346	334	3,4	696	691	0,7
1,91	1,93	1,0	336	325	3,4	643	626	2,5
1,80	1,79	0,8	325	313	3,6	585	559	4,4
1,68	1,66	1,7	309	297	3,8	520	492	5,4
1,56	1,52	2,8	288	281	2,4	450	427	5,2
1,42	1,39	1,9	264	264	0,0	376	369	1,9
1,27	1,27	0,4	237	241	2,0	302	306	1,5
1,11	1,11	0,1	204	202	1,1	227	225	1,0
0,96	0,99	2,9	167	167	0,0	160	165	2,9
Ave. diff %		1,9	Ave. diff %		2,2	Ave. diff %		2,8
Std. dev.		1,3	Std. dev.		1,3	Std. dev.		1,6

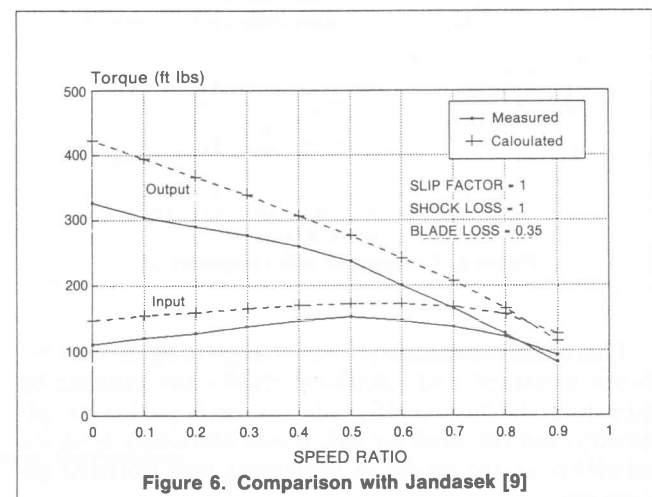
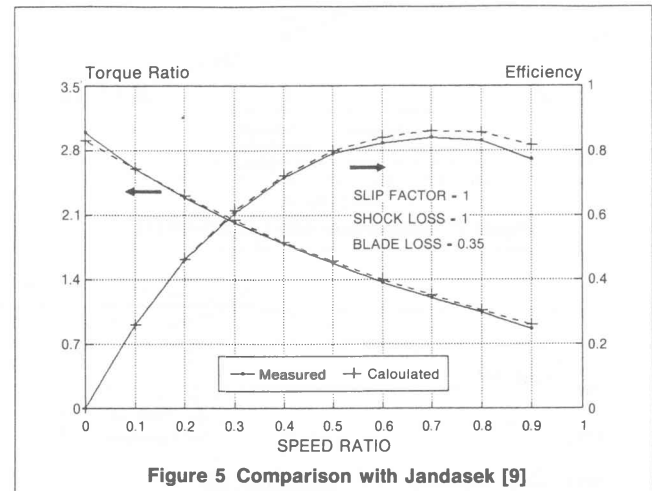
Table 1 Comparison of measured and calculated results for Jandasek [9] torque converter.

tween the calculated and measured values of input and output torque, although this could be improved by changing the shock loss factor to 0.8.

Jandasek [9] did systematic tests on the influence of torque converter geometry on performance, and in one test the impeller blade outlet angle, was changed from



-15° to +55°, increasing the stall torque ratio from 2.1 to 2.99 and reducing both the peak efficiency and coupling point speed ratio. Particularly good agreement was obtained for torque ratio and efficiency, fig. 5, while fig. 6 shows that there was once again only qualitative agreement for input and output torque for this arrangement, using the original loss coefficients and shock loss and slip factors. Reducing the shock loss factor to 0.8 only had a small effect on the results.



Comparisons were also made between the calculated values of the model and measured results obtained from other publications, namely Lucas [10], and Northern Research and Engineering Corporation (NREC) [11]. Reasonable agreement was obtained, Strachan [12], with all these results with varying values of the loss coefficients and shock loss and slip factors.

A comparison was also made against the measured results of the torque converter tested by Lamprecht [7]. This had a two stage turbine, and so for calculation purposes, assigned loss coefficients were split equally between the two turbine stages, being 0.175 each, with impeller and stator assigned loss coefficients of 0.35. Initially a shock loss factor of 0.8 was used, while the slip factor was 0.85, as used by Lamprecht [7]. (the Stanitz [14] formula gives a value of slip factor for this configuration of 0.84) Poor agreement was obtained initially, but this was improved by utilising a shock loss factor of 0.5, figs 7 and 8.

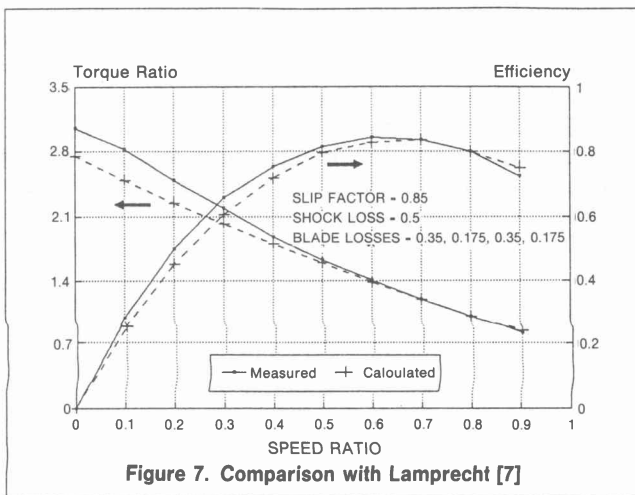


Figure 7. Comparison with Lamprecht [7]

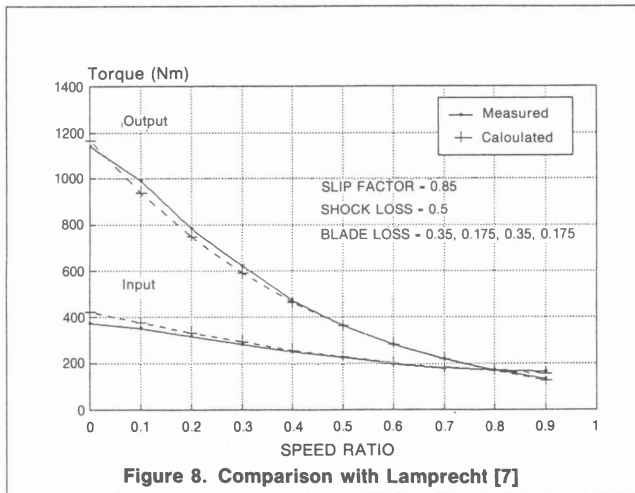


Figure 8. Comparison with Lamprecht [7]

This initial evaluation showed that good agreement between measured and calculated results was possible by adjusting the loss coefficients for each particular geometry, but the need for this would obviously limit the reliability of the model in evaluating new untested geometries.

Model Development

In order to overcome the need to utilise assigned values for the loss coefficient and slip and shock loss factors the model was modified to calculate these values for the impeller, turbine, stator and channels using standard pipe and turbomachinery theory.

Friction, diffusion and profile losses

For pipes, the generally used equation to calculate the friction loss is the Colebrook equation which includes the roughness factor, Giles [13],

$$\frac{1}{\sqrt{\Lambda}} = -2 \times \log\left(\frac{2,51}{\text{Re} \times \sqrt{\Lambda}}\right) + \left(\frac{k_s}{3,7 \times D_h}\right) \quad (1)$$

where Re = Reynolds number based on the pipe or channel hydraulic diameter.

The above expression is difficult to use due to the presence of the friction loss coefficient on both sides of the equation. However a suitable explicit formula for the friction factor of a turbulent pipe has been published, Haaland [15], as;

$$\frac{1}{\sqrt{\Lambda}} = -1,8 \times \log\left[\left(\frac{6,9}{\text{Re}}\right) + \left(\frac{k_s}{3,7 \times D_h}\right)^{1,11}\right] \quad (2)$$

While eq (2) can be applied to the impeller, channel flow was assumed in the casing between the elements, and the casing friction loss coefficient used was the approximation by White [17],

$$k_{(k_s=0)} = -0,495(\log \text{Re}_c)^{-2,2}$$

The casing friction loss coefficient was modified to take into account the effect of roughness by assuming that the ratio of the casing friction loss k, with and without the roughness factor is equivalent to the ratio of the Colebrook equation, with and without the roughness factor. i.e.

$$\frac{k_{(k_s=0)}}{k_{(k_s)}} = \frac{\Lambda_{(k_s=0)}}{\Lambda_{(k_s)}} = \left(\frac{1}{f(\text{Re}, 0)} / \frac{1}{f(\text{Re}, k_s)}\right)^2 \quad (3)$$

Diffusion losses, due to the high deflection of the working fluid, were accounted for by means of the simplified form of the NACA diffusion factor D given by Cohen, Rogers and Saravanamuttoo [16] as

$$D = 1 - \frac{V_1}{V_2} + \left(\frac{\Delta C_w}{2V_1}\right) \cdot \frac{s}{c} \quad (4)$$

The value of D above can be used in conjunction with fig. 5.8, Cohen et al [16] to determine the losses.

Primary losses or profile losses at the design point for the turbine and stator were determined by a method proposed by Ainley and Mathieson [19] whereby the primary loss coefficient at zero incidence ($i = 0$) is given by

$$Y_{p(i=0)} = \left[Y_{p(\alpha_d=0)} + \left(\frac{\alpha_d}{\beta} \right) (Y_{p(\alpha_d=0)} - Y_{p(\alpha_d=0)}) \right] \left(\frac{t}{0,2c} \right)^{\left(\frac{-\alpha_d}{\beta} \right)} \quad (5)$$

where $Y_{p(\alpha_d=0)}$ and $Y_{p(\alpha_d=\beta)}$ are the profile loss coefficients from fig. 3.22(a) and (b), Dixon [18], respectively. At any other incidence, the profile loss ratio $Y_p/Y_{p(i=0)}$ is assumed to be defined by a unique function of the ratio, incidence/stalling incidence, i/i_s , from fig. 3.21 in Dixon [18].

Secondary losses arise from complex three dimensional flows – Dixon [18] states that possibly end wall boundary layers are convected inwards along the suction surface of the blades as the main flow passes through the blade row, resulting in a serious maldistribution of the flow, with losses in the stagnation pressure often a significant part of

the total loss. Ainley and Mathieson [19] determined an expression for the secondary losses, but Dunham and Came [20] found that this equation was not correct for blades of low aspect ratio and modified the expression to include a better correlation with aspect ratio. The loss coefficient can thus be determined from

$$Y_s = 0,1336 \left(\frac{c}{H} \right) \left(\frac{\cos^3 \beta}{\cos \alpha_d} \right) \frac{(\tan \alpha - \tan \beta)^2}{\cos \alpha_m} \quad (6)$$

Depending upon the blade loading, the number of blades and the size and nature of the clearance gap, the tip clearance loss coefficient Y_k can be found from

$$Y_k = B \left(\frac{c}{H} \right) \left(\frac{k_e}{c} \right)^{0,78} \cdot Z_1 \quad (7)$$

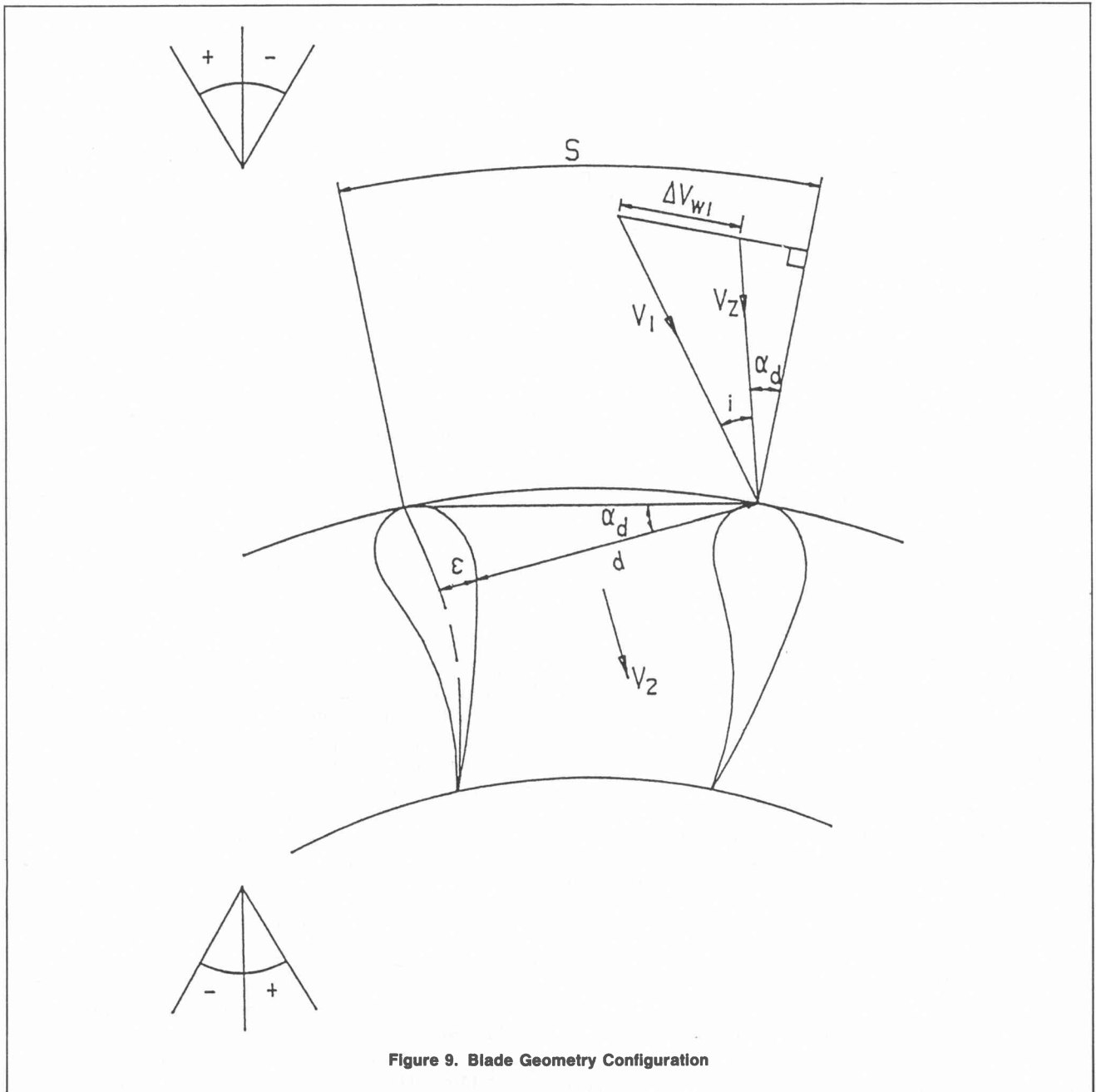


Figure 9. Blade Geometry Configuration

where $B = 0,5$ for unshrouded tips or $0,25$ for shrouded tips and the blade loading is calculated from the secondary loss coefficient, i.e.

$$Z_1 = Y_s \left(\frac{1}{0,0334} \right) \left(\frac{h}{c} \right) \left(\frac{\cos \alpha}{\cos \beta} \right) \quad (8)$$

Ainley and Mathieson [19] obtained their data for a mean Reynolds number of 2.10^5 based on the mean chord and exit flow conditions from the turbine stage. Consequently they recommended a correction to be made to the stage efficiency for lower Reynolds numbers. Dunham and Came [20] gave an optional correction which could be applied directly to the sum of the profile, Y_p , secondary, Y_s , and tip clearance, Y_k , losses as follows;

$$(Y_p + Y_s + Y_k)_{\text{Corrected}} = (Y_p + Y_s + Y_k) \left(\frac{2 \cdot 10^5}{\text{Re}} \right)^{0.2} \quad (9)$$

Shock (incidence) losses

A shock loss factor, for the impeller, turbine and stator, to take into account the difference between the flow angle and blade inlet angle was calculated, Reynaud [22], using the analogy of Vavra's [21] deduction for supersonic shock losses. However, contrary to Vavra [21] and Lamprecht [7], the calculation takes the blade thickness and curvature into account. Fig. 9 shows the blade geometry.

The shock loss coefficient is defined as the total pressure drop between the inlet and outlet of the control volume, fig. 9, divided by the dynamic pressure at outlet from the control volume. i.e.

$$\delta = \frac{p_{t_1} - p_{t_2}}{\frac{1}{2} \cdot \rho \cdot V_2^2} \quad (10)$$

and substituting for the total pressures

$$\delta = \frac{p_{s_1} - p_{s_2} + \frac{1}{2} \cdot \rho \cdot (V_1^2 - V_2^2)}{\frac{1}{2} \cdot \rho \cdot V_2^2} \quad (11)$$

From consideration of the momentum equation for the component perpendicular to the control volume outflow boundary

$$p_{s_1} \cdot s \cdot \cos \alpha_d - p_{s_2} \cdot d - \frac{1}{2} \cdot \epsilon \cdot (p_{s_2} + p_{s_1}) = \dot{m} \cdot V_2 - \dot{m} \cdot V_1 \cdot \cos i \quad (12)$$

where $d = s \cdot \cos \alpha_d - \epsilon$ and \dot{m} is the mass flow rate per blade channel. It is assumed that the pressure acting on the blade surface forming the boundary of the control volume is equal to the mean of the pressure at the inlet and outlet of the control volume.

From the continuity equation;

$$\dot{m} = \rho \cdot s \cdot V_1 \cdot \cos (\alpha_d + i) = \rho \cdot d \cdot V_2 \quad (13)$$

and since $V_2 = k \cdot V_1$ the value of k can be calculated as

$$k = \frac{V_2}{V_1} = \frac{s}{d} \cdot \cos (\alpha_d + i) \quad (14)$$

Substituting for d , \dot{m} and V_2 into eq (12)

$$p_{s_1} \cdot \left(s \cdot \cos \alpha_d - \frac{\epsilon}{2} \right) - p_{s_2} \cdot \left(s \cdot \cos \alpha_d - \epsilon + \frac{\epsilon}{2} \right) = \rho \cdot d \cdot k \cdot V_1^2 \cdot \cos i - \rho \cdot d \cdot k^2 \cdot V_1^2$$

Rearranging

$$p_{s_1} - p_{s_2} = \frac{d}{s} \cdot \rho \cdot k \cdot V_1^2 \cdot \left(\frac{k - \cos i}{\cos \alpha_d - \frac{\epsilon}{2s}} \right) \quad (15)$$

and substituting eq (15) into eq (11)

$$\delta = \frac{\frac{d}{s} \cdot \rho \cdot k \cdot V_1^2 \cdot \left(\frac{k - \cos i}{\cos \alpha_d - \frac{\epsilon}{2s}} \right) + \frac{1}{2} \cdot \rho \cdot V_1^2 \cdot (1 - k^2)}{\frac{1}{2} \cdot \rho \cdot V_1^2 \cdot k^2}$$

and rearranging again

$$\delta = \frac{k^2 \left(\frac{2d}{s \left(\cos \alpha_d - \frac{\epsilon}{2s} \right)} - 1 \right) - 2 \cdot k \cdot \cos i \cdot \left(\frac{d}{s \left(\cos \alpha_d - \frac{\epsilon}{2s} \right)} \right) + 1}{k^2} \quad (16)$$

For thin straight blades, this reduces to

$$\delta = \frac{(V_2^2 - 2 \cdot V_2 \cdot V_1 \cdot \cos i + V_1^2)}{V_2^2}$$

Referring to fig 9 and using the definition of k and the Cosine rule it can be shown that

$$\delta = \frac{\Delta V_{w1}^2}{V_2^2} \quad (17)$$

Therefore, equating eqs (10) and (17)

$$p_{t_1} - p_{t_2} = \frac{1}{2} \cdot \rho \cdot \Delta V_{w1}^2$$

Thus the equation utilised by Lamprecht [7] is equivalent to the common assumption used by Lucas [2], Whitfield et al [5] and Adrian [8], i.e. that the incidence loss is equal (or at least proportional) to the dynamic pressure associated with the difference between the design and actual relative circumferential velocity component. The incidence loss model, eq (16) above, may thus be regarded as a generalisation of a commonly used model applied to thick, curved blades.

Slip Factor

Even under ideal frictionless conditions, the relative flow leaving a compressor or pump impeller receives less than perfect guidance, and the flow is said to slip. Several methods of determining the slip factor are available in the literature and Lamprecht [7] used the Stanitz [14] method which Dixon [18] states as being suitable for radial vaned impellers ($\beta_d = 0$). For impellers having blade angles in

the range $50^\circ < \beta_d < 70^\circ$, Dixon [18] recommends either the Stodola or Busemann formulas. Wiesner [23] carried out a comprehensive review of published slip factors and found that the Busemann formula gave best agreement with test slip factors determined from measured results. Wiesner [23] further recommended a simple empirical function that correlated very well with the test results, namely;

$$\sigma = 1 - \frac{\sqrt{\cos \beta_d}}{Z_n^{0.7}} \quad (18)$$

This is only applicable within the following limits

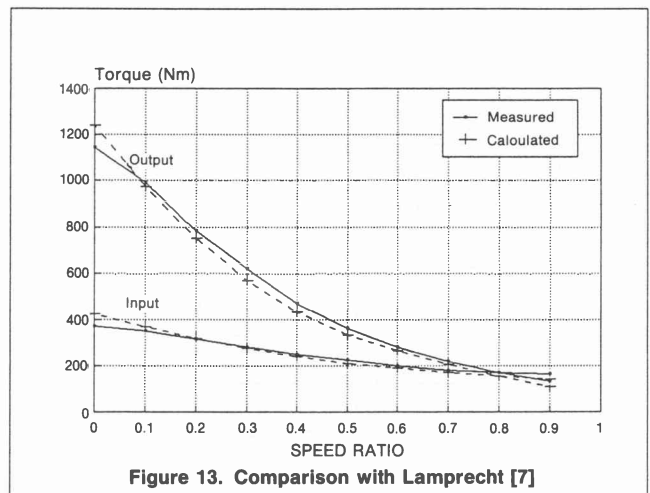
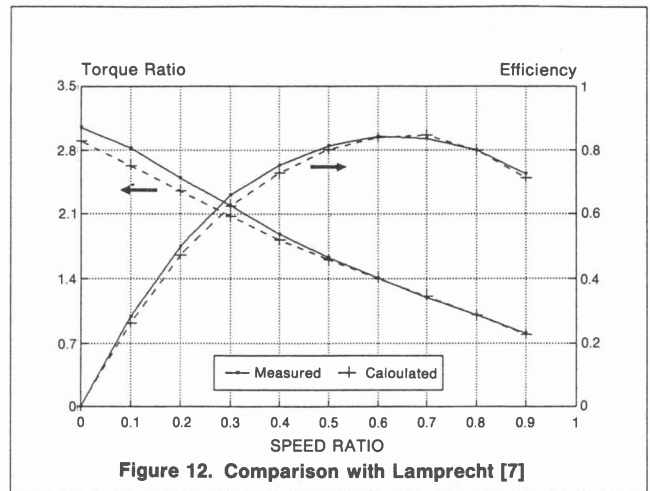
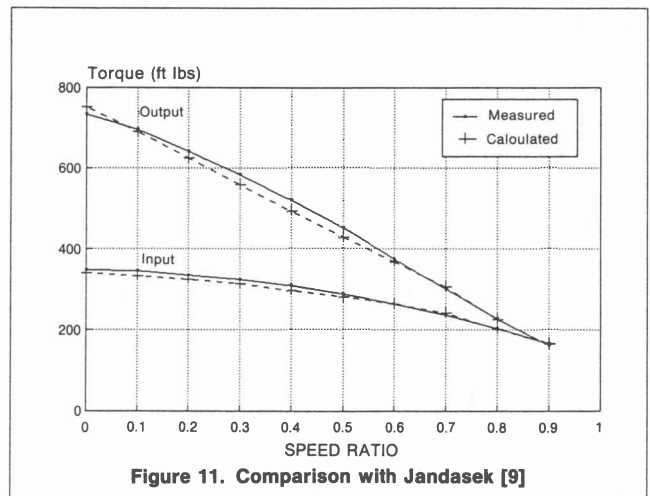
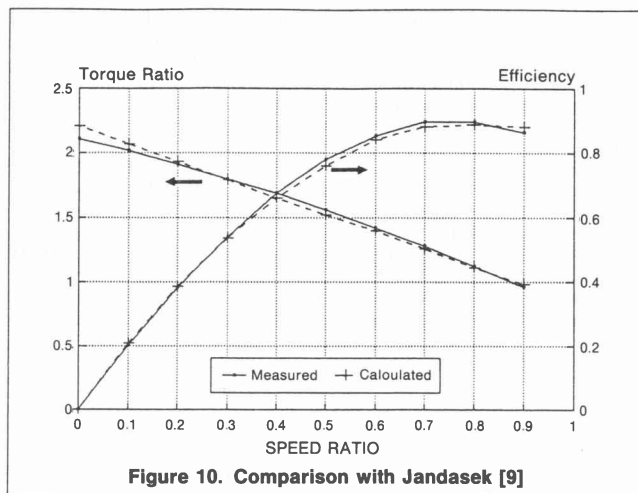
$$\frac{r_1}{r_2} \leq \frac{1}{\exp\left(\frac{8,16 \cdot \cos \beta_d}{Z_n}\right)} = \epsilon_{Lim}$$

For a radius ratio in excess of the above limit the slip factor is given by;

$$\sigma = \left(1 - \frac{\sqrt{\cos \beta_d}}{Z_n^{0.7}}\right) \left[1 - \left(\frac{\frac{r_1}{r_2} - \epsilon_{Lim}}{1 - \epsilon_{Lim}}\right)^3\right] \quad (19)$$

Discussion

For the above calculations, the computer model required more detailed data than that given in most publications. However, of the literature already studied, both Lamprecht [7], and Jandasek [9] gave sufficient information to satisfy the input requirements of the model, and figs 10 and 11 show the comparison of measured and calculated results for the Jandasek [9] torque converter using the latest version of the model. When compared to figs. 3 and 4 a significant improvement is apparent. Table 1 lists the numerical values of measured and calculated torque ratio, efficiency, and input and output torque for figs 3 and 4, and figs 10 and 11, and the reductions in the mean and standard deviations of the errors between the two versions of the model are significant. Comparative results for the Lamprecht [7] geometry using the loss models are shown in figs 12 and 13, and compare favourably with



figs 7 and 8, for the same torque converter, but where arbitrary values were used for the loss coefficients. Table 2 shows the numerical values for these sets of figures and the efficacy of the loss models to simulate the torque converter over the whole operating range is apparent.

Conclusion

From the foregoing it can be seen that the performance of the torque converter hydrodynamic model has been systematically improved by the introduction of empirical

(a) Figs. 7 and 8

Torque Ratio			Input Torque Nm			Output Torque Nm		
Meas	Calc	Diff %	Meas	Calc	Diff %	Meas	Calc	Diff %
3,05	2,75	9,8	374	424	13,2	1142	1166	2,1
2,82	2,49	11,7	350	376	7,3	990	939	5,2
2,49	2,25	9,7	315	333	5,7	784	748	4,5
2,20	2,02	8,0	283	293	3,5	622	592	4,8
1,88	1,88	4,4	251	257	2,4	473	463	2,1
1,63	1,63	2,3	224	228	1,8	364	362	0,5
1,41	1,41	1,9	200	204	2,0	281	281	0,0
1,20	1,20	0,2	182	184	1,1	218	220	0,9
1,00	1,00	0,0	170	168	1,2	170	168	1,2
0,81	0,83	3,2	164	154	6,0	133	129	3,0
Ave. diff %		11,36	Ave. diff %		4,4	Ave. diff %		2,4
Std. dev.		8,44	Std. dev.		3,6	Std. dev.		1,8

(b) Figs 12 and 13

Torque Ratio			Input Torque Nm			Output Torque Nm		
Meas	Calc	Diff %	Meas	Calc	Diff %	Meas	Calc	Diff %
3,05	2,90	4,9	374	428	14,3	1142	1241	8,7
2,83	2,63	7,1	350	370	5,6	990	972	1,8
2,49	2,35	5,5	315	319	1,3	784	750	4,3
2,20	2,08	5,3	283	275	2,8	622	572	8,0
1,88	1,82	3,4	251	240	4,7	473	436	7,9
1,63	1,60	1,5	224	210	6,2	364	337	7,6
1,41	1,40	0,7	200	190	5,0	281	265	5,6
1,20	1,21	1,1	182	170	6,5	218	206	5,5
1,00	1,00	0,0	170	154	9,3	170	154	9,3
0,81	0,79	1,9	164	143	13,3	133	113	14,9
Ave. diff %		3,1	Ave. diff %		6,9	Ave. diff %		7,4
Std. dev.		2,3	Std. dev.		4,0	Std. dev.		3,3

Table 2 Comparison of measured and calculated results for Lamprecht [7] torque converter.

loss models from the literature and an original incidence loss model which takes blade thickness into account. The relative accuracy and shape of the predicted performance curves in figs 10 to 13 show that the loss models are realistic when applied to two significantly different commercial torque converter geometries and the model can now be confidently used as a preliminary design tool for predicting torque converter performance. Application of the model requires detailed geometry data and as this is not generally available from the literature further comparisons between the model and measured results cannot easily be made.

Further development of the loss models is not considered necessary although one area for future investigation is possibly the effect of fluid temperature on torque converter performance.

References

1. SAE Recommended Practices, Hydraulic Drives Terminology, SAE J641, SAE Handbook 1983
2. Lucas G. G., and Rayner, A. A. "Torque converter design calculations", Automobile Engineer, February 1970
3. Qualman, J. W. and Egbert, E. L., "Fluid couplings", Passenger Car Automatic Transmission, SAE Transmission Workshop Meeting, 2nd Edition, Advanced Engineering, Vol 5, pp 137-150, 1963
4. Walker, F. H., "Multi-turbine torque converter", Design Practices Passenger Car Automatic Transmissions, 2nd Edition, pp 227-240, Society of Automotive Engineers, 1973
5. Whitfield, A., Wallace, F. J., and Patel, A. "Design of three element hydrokinetic torque converters", Int. J. Mech. Sci., Vol 25, No. 7, pp 485-497, 1983
6. Wallace, F. J., Whitfield, A., and Sivalingam, R. "A performance prediction procedure for three element torque converters", Int. J. Mech. Sci., Vol 20, pp 801-814, 1978
7. Lamprecht, J., "Die ontwerp van 'n hidrouliese wringomsetter", Magister tesis in Ingenieurswese, Universiteit van Pretoria, Desember 1983
8. Adrian, F-W., "Strömungsuntersuchungen und analyse in kreisläufen hydrodynamischer wandler.", Doctorarbeit, Ruhr-Universität Bochum, 1985
9. Jandasek, V. J., "The design of a single stage three-element torque converter", Passenger Car Automatic Transmission, SAE Transmission Workshop Meeting, 2nd Edition, Advanced Engineering Vol 5, p 201, 1963
10. Lucas, G. G., "A technique for calculating the time-to-speed of an automatic transmission vehicle.", Proc. I. Mech. E., Vol. 184, Part 31, 1969
11. Northern Research and Engineering (NREC), "Modification of torque converter analysis procedures", NREC Report No. 1152.1, Northern Research and Engineering Corporation, Cambridge, Mass, USA, March 1969
12. Strachan, P. J., "Torque converter one-dimensional computer program: Comparison of calculated input and output torque with experimental values." BMI Confidential Report 85/15/86/020, March 1987
13. Giles, R. V., "Theory and Problems of Fluid Mechanics and Hydraulics", Schaum's Outline Series, Schaum Publishing Co., New York, 1963
14. Stanitz, J. D., "Some theoretical aerodynamic investigations of impellers in radial and mixed flow centrifugal compressors.", Trans. A.S.M.E., 74, 4, 1952
15. Haaland, S. E., "Simple and explicit formulas for the friction factor in turbulent pipe flow," ASME Journal of Fluids Engineering, Vol. 105, 1983, pp 89-90
16. Cohen, H., Rogers, G. F. C. and Saravanamuttoo, H. I. H., "Gas Turbine Theory", Longman Scientific and Technical, 3rd Edition, 1987
17. White, F. M., "Viscous Fluid Flow", McGraw-Hill, 1974
18. Dixon, S. L., "Fluid Mechanics, Thermodynamics of Turbomachinery", 3rd Edition, Pergamon International Library, 1984
19. Ainley D. G. and Mathieson, G. C. R., "A method of performance estimation for axial flow turbomachines", A.R.C.R. and M. 2974, 1951
20. Dunham, J. and Came, P., "Improvements to the Ainley-Mathieson method of turbine performance prediction", Trans. A.S.M.E., Series A., 92, 1970
21. Vavra, M. H., "Aero-Thermodynamics and Flow in Turbomachines", Kriege, New York, 1974
22. Reynaud, F. P., "BMI one-dimensional torque converter model", BMI Confidential Report 88/28, March 1990
23. Wiesner, F. J., "A review of slip factors for centrifugal impellers.", Journal of Engineering for Power, Trans. of the ASME, Oct. 1967